Brain Structure and Function (2019) 224:907–923
https://doi.org/10.1007/s00429-018-1812-0

ORIGINAL ARTICLE

Structure, asymmetry, and connectivity of the human temporo-parietal aslant and vertical occipital fasciculi

Sandip S. Panesar[1] · Joao Tiago A. Belo[2] · Fang-Cheng Yeh[2,3] · Juan C. Fernandez-Miranda[1]

Received: 28 November 2017 / Accepted: 4 December 2018 / Published online: 12 December 2018

Abstract

We previously proposed a bipartite 'dorsal–ventral' model of human arcuate fasciculus (AF) morphology. This model does not, however, account for the 'vertical,' temporo-parietal subdivision of the AF described in earlier dissection and tractographic studies. In an effort to address the absence of the vertical AF (VAF) within 'dorsal–ventral' nomenclature, we conducted a dedicated tractographic and white-matter dissection study of this tract and another short, vertical, posterior-hemispheric fascicle: the vertical occipital fasciculus (VOF). We conducted atlas-based, non-tensor, deterministic tractography in 30 single subjects from the Human Connectome Project database and verified our results using an average diffusion atlas compiled from 842 separate normal subjects. We also performed white-matter dissection in four post-mortem specimens. Our tractography results demonstrate that the VAF is, in fact, a bipartite system connecting the ventral parietal and temporal regions, with variable connective, and no volumetric lateralization. The VOF is a non-lateralized, non-segmented system connecting lateral occipital areas with basal–temporal regions. Importantly, the VOF was spatially dissociated from the VAF. As the VAF demonstrates no overall connective or volumetric lateralization, we postulate its distinction from the AF system and propose its re-naming to the 'temporo-parietal aslant tract,' (TPAT), with unique dorsal and ventral subdivisions. Our tractography results were supported by diffusion atlas and white-matter dissection findings.

Introduction

The anatomy, classification, and even existence of posterior-hemispheric association white-matter tracts have been subject to controversy in the neuroanatomical literature. In the tractography era, fiber dissection descriptions of the AF included a subcomponent known as the 'vertical arcuate fasciculus', which comprised one of three AF subcomponents (Catani et al. 2002, 2005; Fernández-Miranda et al. 2008). The 'vertical AF' (VAF) was described as a short, vertically oriented tract originating within the posterior temporal lobe and terminating within the inferior parietal cortex. Along with the fronto-parietal horizontal subcomponent, it formed the 'superficial-AF,' which lay superficial to a long temporo-frontal perisylvian component to comprise the 'AF' in its entirety. Proponents of this original description (Catani and Thiebaut de Schotten 2008; Thiebaut de Schotten et al. 2011; Martino et al. 2013a, b; Martino and García-Porrero 2013) regard the AF as part of the greater superior longitudinal fasciculus (SLF) system, with the AF proper referred to as the 'perisylvian-SLF' or 'SLF-IV.' Recent fiber dissection and tractographic studies have questioned this description: instead, the AF has been shown to be a purely temporo-frontal tract, with a 'dorsal–ventral' arrangement and without any temporo-parietal or fronto-parietal connectivity (Lawes et al. 2008; Rilling et al. 2008; Glasser and Rilling 2008; Fernández-Miranda et al. 2015). This view, however, contradicts postulations of the AF and SLF belonging to the same fiber system: In this model, the AF, but not the SLF, is strongly leftward lateralized in connectivity and volumetry. Further studies have demonstrated the SLFs' rightward-tending connectivity and volumetric lateralization (Thiebaut de Schotten et al. 2011; Wang et al. 2016). This

Electronic supplementary material The online version of this article (https://doi.org/10.1007/s00429-018-1812-0) contains supplementary material, which is available to authorized users.

✉ Juan C. Fernandez-Miranda
drjfm@stanford.edu

[1] Department of Neurosurgery, Stanford University, 300 Pasteur Drive Palo Alto, 94304 California, USA

[2] Department of Neurological Surgery, University of Pittsburgh, Pittsburgh, PA, USA

[3] Department of Bioengineering, University of Pittsburgh, Pittsburgh, PA, USA

dorsal–ventral AF argument leaves the previously described VAF unaccounted for among the oppositely lateralized AF/SLF arrangement. Recent tractography-derived description of the frontal-aslant tract (FAT) (Catani et al. 2012, 2013) demonstrates that short, low-volume white-matter systems, previously obscure to post-mortem fiber dissection techniques, can be reliably studied using tractography. Furthermore, limitations of the early tractographic techniques [i.e., diffusion tensor imaging (DTI)] including the inability to trace crossing fiber pathways (Farquharson et al. 2013) could be better addressed by a more advanced reconstruction algorithm (Yeh et al. 2010). Recent efforts have been made using both DTI and high-angular resolution methods to further elucidate the place of the VAF amongst the AF and SLF systems, with plenty of controversy, for example the existence of the so-called 'temporo-parieto-occipital' (TPO) component (Martino et al. 2013a; Bartsch et al. 2013; Martino and García-Porrero 2013; Kamali et al. 2014a, b; Martino and De Lucas 2014; Wu et al. 2016). Nevertheless, these studies were only conducted in small-volume subject sets. Despite modern tractography algorithms being generally able to distinguish the VAF from neighboring structures, controversies pertaining to its subdivision, laterality, and connectivity remain.

Another short, vertical tract known as the vertical occipital fasciculus (VOF) is a connection within the extreme-posterior hemisphere. It was first described towards the end of the nineteenth century. Its description disappeared from neuroanatomical literature until the introduction of autoradiographic and tractographic techniques from the 1970s onwards (Yeatman et al. 2013, 2014; Takemura et al. 2016, 2017; Güngör et al. 2017; Weiner et al. 2017). A dedicated study by Yeatman et al. (2013) defined the anatomy of the posterior visual word-form area, and tractographically reproduced this bundle. The authors described a tract ascending from the occipito-temporal sulcus, lateral to the inferior longitudinal fasciculus (ILF) which terminated within the parieto-occipital association cortices. Since then, several tractographic studies into VOF anatomy have been conducted using both DTI and high-angular resolution methods (Martino and De Lucas 2014; Bouhali et al. 2014; Keser et al. 2016; Takemura et al. 2016). Nevertheless, relative to the well-known larger association fascicles, little data exist pertaining to the VOFs subdivision, connectivity, and lateralization.

With these considerations, we conducted a dedicated tractographic and white-matter dissection study into the morphology, volumetry, and connectivity of the VAF and VOF in an effort to address several issues: (1) The missing VAF in the contemporary 'dorsal–ventral' AF model. (2) Apply a deterministic non-tensor tractographic algorithm to address the issue of discreet or unified VAF and VOF as highlighted by Weiner et al. (2017). (3) Specifically, analyze the lateralization of the VAF to determine whether it yielded further evidence for the argument regarding dissociation of the AF and SLF systems in the contemporary literature. (4) Further analyze the 'temporo-parieto-occipital' (TPO) component as proposed by Kamali et al. (2014a, b) and Wang et al. (2016).

Methods

Three principal methods were used in this study: first, a dedicated subject-specific study was conducted in 30 healthy, individual subjects, along with a diffusion tractography atlas consisting of averaged diffusion data from 842 individual subjects for verification. Finally, both tractographic methods were complemented by a white-matter dissection study in post-mortem brains.

Participants

We conducted a subject-specific deterministic fiber tractography study in 30 right-handed, neurologically healthy male and female subjects, age range 23–35. The data were from the Human Connectome Project (HCP) online database WU-Minn Consortium (Principal Investigators: David van Essen and Kamil Ugurbil; 1U54MH091657) funded by the 16 NIH institutes and centers that support the NIH Blueprint for Neuroscience Research and by the McDonnell Center for Systems Neuroscience at Washington University. Likewise, data from 842 individual HCP subjects were utilized to compile the averaged diffusion atlas.

Image acquisition and reconstruction

The HCP diffusion data for individual subjects were acquired using a Siemens 3T Skyra system, with a 32-channel head coil (Siemans Medical, Erlangen, Germany). A multishell diffusion scheme was used, and the *b* values were 1000, 2000, and 3000s/mm^2. The number of diffusion sampling directions was 90, 90, and 90, respectively. The in-plane resolution and slice thickness were both 1.25 mm (TR = 5500 ms, TE = 89 ms, resolution = 1.25 mm × 1.25 mm, FoV = 210 mm × 180 mm, matrix = 144 × 168). The raw diffusion data were downloaded from the HCP public database and reconstructed by us using the generalized q-sampling imaging approach (Yeh et al. 2010), using a diffusion distance ratio of 1.2 as recommended by the original study.

HCP 842 atlas

A total of 842 participants from the HCP database were used to construct the atlas (Yeh et al. 2018) (available at http://

dsi-studio.labsolver.org). The image acquisition parameters are identical to those in 2.2. The diffusion data from the participants were reconstructed and warped to the Montreal Neurological Institute (MNI) space using q-space diffeomorphic reconstruction (Yeh and Tseng 2011) with a diffusion sampling length ratio of 1.25 and an output resolution of 1 mm. The group average atlas was then constructed by averaging the reconstructed data of the 842 individual subjects within the MNI space. Our atlas methodology has been explained in a recent, dedicated study (Yeh et al. 2018).

Fiber tracking and analysis

We performed deterministic fiber tracking using DSI Studio software, which utilizes a generalized streamline fiber tracking method (Yeh et al. 2013). Parameters selected for fiber tracking included a step size of 0.2 mm, a minimum fiber length of 20 mm, and a turning angle threshold of 60°. For progression locations containing > 1 fiber orientation, fiber orientation most congruent with the incoming direction and turning angle < 60° was selected to determine subsequent moving direction. Each progressive voxels' moving directional estimate was weighted by 20% of the previous voxels' incoming direction and by 80% of it is nearest fiber orientation. This sequence was repeated to create fiber tracts. Termination of the tracking algorithm occurred when the quantitative anisotropy (QA) (Yeh et al. 2013) dropped below a subject-specific, pre-selected threshold value of between 0.02 and 0.08, when fiber tract continuity no longer met the progression criteria or when 100,000 tracts were generated. We pre-selected QA termination threshold by analyzing the number of false continuations generated within each subject's data set and chose the compromise value that allowed optimal anatomical detail with minimal noise. Likewise, we selected a smoothing parameter of 50% for the same reason stated previously.

To generate the desired tracts, we employed an atlas-based approach (Fernández-Miranda et al. 2015; Wang et al. 2016; Panesar et al. 2017), along with manually placed regions of interest (ROIs) and regions of avoidance (ROAs). We utilized the Automated Anatomical Labeling atlas (AAL) (Tzourio-Mazoyer et al. 2002) to select cortical seeding regions. Briefly, the AAL regions were warped to each individual subject' diffusion matrix using the linear and non-linear registration algorithm feature in DSI Studio. This feature allows the alignment of pre-defined cortical atlas regions to each subject's unique diffusion map. This results in optimal atlas region placement, requiring little-to-no manual manipulation. For the VAF, we chose parietal regions, as parcellated by the AAL atlas: precuneus (Pc), superior parietal lobule (SPL), and inferior parietal lobules [dorsal and ventral aspects of the supramarginal gyrus (dSmG; vSMG) and angular gyrus (AG)]. A rectangular axial ROI was placed ventral to the seeding regions in the axial plane, to select only fibers passing dorsal–ventral (i.e., parietal–temporal/parietal–occipital). An additional cross-shaped rectangular ROA was utilized, with one portion lying in the coronal plane and one in the sagittal plane. The coronal ROA was to prevent any anteriorly traveling fibers (i.e., AF/SLF/cingulum components) from being generated, and the sagittal ROA was used to prevent any of the commissural fibers from being generated. VOF fibers were generated separately. Three ventral occipital gyri were chosen for generating the VOF: [superior occipital gyrus (SO); middle occipital gyrus (MO); cuneus (Cu)]. The same rectangular ROI was utilized but moved ventral relative to its positioning for VAF generation (Fig. 1a, b). The process was repeated for both right and left hemispheric vertical AFs and VOFs. The chosen atlas-based approach to fiber tracking was to ensure the consistency of methodology across subjects, with minimal permitted a priori or inter-user variability. Once 100,000 fiber tracts had been generated, we manually selected fibers traveling parieto-temporally, parieto-occipitally, occipito-occipitally, or occipito-temporally for further analysis. We subsequently analyzed the dorsal and ventral morphology and connectivity of each bundle for connectivity analysis.

Defining cortical terminations

We utilized the "endpoints-to-ROI" function in DSI studio to visualize the dorsal and ventral connectivity profiles of each bundle. This converts fiber endpoints into larger cortical areas for better visualization. The endpoint ROIs were then manually compared by superimposing specific AAL atlas regions to analyze tract origination/termination patterns. This was done for the VAF and VOF in all 30 subjects, with left and right connectivity patterns being noted. We used the percentage frequency of an observed connection across the 30 subjects of our subject-specific as an analog of connectivity 'strength,' i.e., the higher the frequency of subjects that a particular connection is observed in, the more likely it is a true connection versus an artifact.

Volumetry and lateralization

We calculated the number of voxels occupied by each fiber trajectory (streamlines) and the subsequent volume (in milliliters) of each vertical AF and VOF. Prior to segmenting the tracts, we utilized the 'delete repeated tracts' function in DSI studio. This automatically removes tracts (at a user-selected threshold) that are substantially close to each other or overlapping. All repeated tracts within 1 voxel of each other were deleted automatically using pre-determined distance metrics (see Yeh et al. 2018). Lateralization index (LI) (Catani et al. 2007) was determined using the formula [(left tract volume × right tract volume) × (left tract volume + Right tract

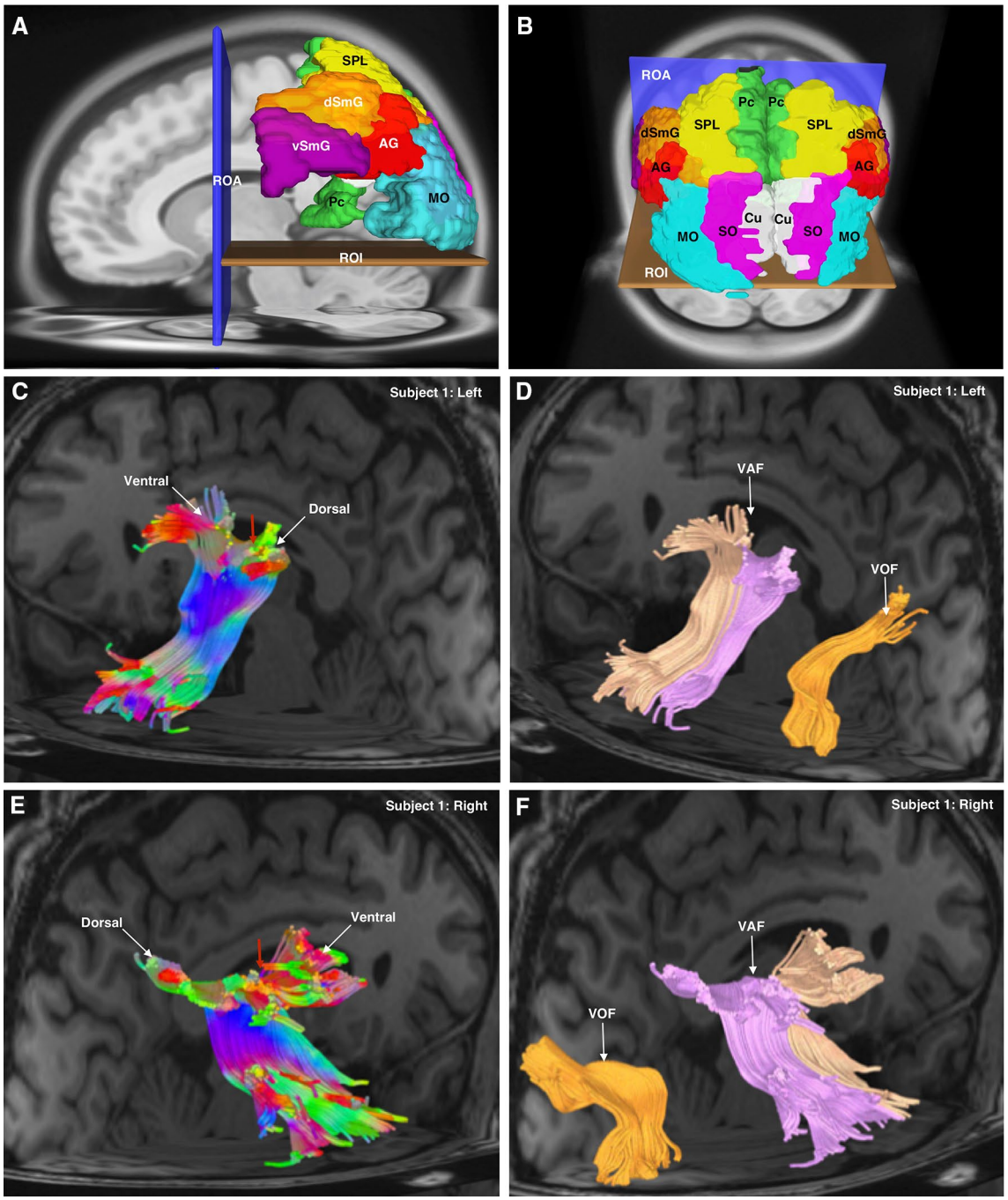

volume)] × 2. This gives an index value between ×2 and +2. LI values around 0 represent general volumetric symmetry between the tracts of the left hemisphere and right hemisphere. Values less than −0.4 or greater than +0.4 represent a significant right hemisphere or left hemispheric volumetric asymmetry, respectively. In addition to calculating LI, the volumes of the left and right vertical AFs and VOFs from the 30 subjects were each subjected to an independent samples *T* test in SPSS (IBM Corporation, Armonk, New York) to calculate the significance of mean hemispheric volumetry over the 30 subjects. To statistically compare the lateralization of the VAF, AF, and SLF, the LI values for each tract across all 30 subjects were subjected to a single-factor ANOVA with post hoc Tukey HSD analysis in SPSS.

Tractography of adjacent fiber systems

To further validate our anatomical study of the VAF, we conducted complementary tractography of the AF and SLF in individual subjects, and the HCP 842. Tracking the AF

◂**Fig. 1** **a** Sagittal view of the left hemisphere using the AAL atlas in the HCP 842 atlas demonstrating the seeding method for both the VAF (TPAT) and VOF. The ROA and ROI were the same for both bundles. For TPAT, supramarginal gyrus, dorsal and ventral portions (dSmG; vSmG), angular gyrus (AG), superior parietal lobule (SPL), and precuneus (PC). For the VOF, the superior occipital (SO; not visible), middle occipital (MO), and cuneus (Cu; not visible) were used. **b** Oblique, superior–posterior view of the seeding method for the VAF and VOF within the HCP 842 atlas. The ROA and ROI were the same for both bundles. For VAF, dorsal (dSmG) and ventral (vSmG) supramarginal gyrus, angular gyrus (AG), superior parietal lobule (SPL), and precuneus (PC). For the VOF, the superior occipital (SO; not visible), middle occipital (MO), and cuneus (Cu; not visible) were used. **c** Posterior-oblique view of left hemisphere in a single subject (Subject 1) from the subject-specific analysis shows the left VAF. Tract colors are directionally assigned. The wedge in the middle (red arrow) demonstrates the plane used to separate the tracts for further analysis. Also indicated are the ventral and dorsal parietal bifurcations of this tract in the parietal lobe. **d** Posterior-oblique view of left hemisphere of Subject 1. The two divisions of the VAF have been colored separately (light orange color for ventral and pink for dorsal) following division, whilst the VOF is also visible (dark orange) and clearly separated from the VAF. **e** Posterior-oblique view of right hemisphere of Subject 1 shows the left VAF. Tract colors are directionally assigned. The wedge in the middle (red arrow) demonstrates the plane used to separate the tracts for further analysis. Also indicated are the ventral and dorsal parietal bifurcations of this tract in the parietal lobe. **f** Posterior-oblique view of right hemisphere of Subject 1. The two divisions of the VAF have been colored separately (light orange color for ventral and pink for dorsal) following division, whilst the VOF is also visible and labeled (dark orange), clearly separated from the VAF

involved placement of seed regions corresponding to the superior (STG), middle (MTG), and inferior (ITG) temporal gyri as represented within the AAL atlas. A single, rectangular ROI was subsequently placed below the seed regions, in the coronal plane, at the approximate level of the fronto-parietal junction. This selected only AF fibers traveling from the temporal-to-frontal regions. The method was derived from Fernandez-Miranda et al. (2015). For the SLF, we utilized AAL seed regions corresponding to the entire parietal lobe, and the same rectangular, coronally lying ROI that was used for AF tracking. This method selected only fibers traveling postero-anteriorly from the parietal lobe. This method was identical to Wang et al. (2016). We analyzed the volume of both the AF and the SLF in their entirety (i.e., non-divided) using the same method as described in 2.6. From these results, we calculated both hemispheric LI and subjected the left and right values to *T* testing in SPSS to calculate the significance of lateralization values. This was repeated across all 30 subjects and within the HCP-842.

White-matter fiber dissection

Two human brain specimens were prepared for dissection. First, they were fixed in a 10% formalin solution for 2 months. After fixation, the arachnoid and superficial vessels were removed. The brains were subsequently frozen at − 16 °C for 2 weeks, as per the Klingler method (Ludwig and Klingler 1956). The dissection commenced 24 h after the specimens were thawed and proceeded in a step-wise, superficial-to-deep process. Dissection was achieved using wooden spatulas to remove successive layers of gray matter and then white matter.

Results

Vertical arcuate fasciculus

Morphology

Tracts resembling the VAF were reproduced successfully in all 30 subjects bilaterally. The fibers of the VAF assumed an 'extended U-fiber' shape, consisting of a compact stem with terminations fanning out at parietal and temporal extremities. The middle-stem portion traveled vertically, approximately at the level of the Sylvian fissure, between the temporal and parietal lobes (Fig. 1c, f). Upon tract generation, we noticed a distinct anterior–posterior bifurcation pattern of the VAF. We segmented whole VAF bundles into two separate tracts by selecting only fibers superior to the bifurcation. As such, we isolated two distinct tracts, which henceforth are referred to as 'ventral VAF (vVAF)' and 'dorsal VAF (dVAF).' These distinct subdivisions of the VAF were each found in 58 out of 60 hemispheres (See also supplementary Figs. 1a–h and 2a–f). This general morphology, including the subdivisions, was also found within the HCP 842 template.

Connectivity

We describe ventral and dorsal connectivity patterns in terms of the vVAF and dVAF. The vVAF predominantly connected to the dorsal and ventral aspects of the SmG, or more anteriorly. Connectivity of the vVAF to SmG was generally consistent in both left (83% of subjects) and right (73% of subjects) hemispheres. Dorsal SmG connectivity of the vVAF was leftward-dominant, with this connection found in 73% of subjects left hemispheres but only 20% of right hemispheres. In addition, minor vVAF connectivity to the AG was found in 30% of left hemispheres and 33% of right hemispheres. Ventrally, the vVAF terminated within the MTG in 97% and 83% of subjects' left and right hemispheres, respectively. vVAF connectivity to the inferior temporal gyrus (ITG) was 43% and 30% on the left and right, respectively. Dorsally, the dVAF connected predominantly with the AG in 70% of subjects on the left and 93% of on the right. There was minor connectivity to ITG on both the left (20%) and right (17%). Temporal connectivity of the dVAF

was hemispherically differentiated: On the left, it predominantly connected with the MTG (80%) and ITG (50%). On the right, however, it connected equally (67%) to the MTG and ITG. No connectivity of either division was found to the superior temporal gyrus (STG), or the basal occipitotemporal gyri [ITG, fusiform (FG), or lingual gyrus (LG)]. Connectivity patterns were identical within the HCP 842 (Fig. 2a, b; Table 1).

Volumetry and lateralization

The mean volume of the left and right VAFs prior to manual separation was 9.7 ml and 9.3 ml, respectively [$n=30$, not significant ($t=0.421$, $p=0.675$)]. Prior to segmenting, we used the 'delete repeated tracts' function in DSI studio to prevent extra tracts contributing artifactually to streamline number. After manual separation, the vVAF had mean left and right hemispheric volumetry of 6.3 ml and 5.3 ml, respectively. Left and right dVAFs were smaller overall, with the right being larger than the left at 4.4 ml vs 3.8 ml. When vVAF and dVAF volumes were added, the mean volumes were 10.1 ml (0.4 ml larger than pre-manual separation) for the left VAF and 9.8 (0.4 ml larger than pre-separation) for the right VAF. Again, the difference between lateralization of the two summated VAFs was not significant ($t=0.470$, $p=0.640$). For non-summated VAF volumes, the LI was 0.04, and for summated volumes was 0.03, representing hemispheric symmetry. On the HCP 842 template, prior to separation, the left and right VAF volumes were 5.9 and 6.9 ml on the right and left, respectively. The left vVAF was 3.9 ml and the dVAF was 2.8 ml, giving a summated volume of 6.7 ml (0.8 ml difference). On the right, volumes were 2.1 and 4.8 ml and 6.9 ml (0.1 ml difference) for the vVAF and dVAF and their sum, respectively. Lateralization indices were 0 for unmerged and −0.1 for merged VAF bundles (Table 2).

Vertical occipital fasciculus

Morphology

Vertically oriented extreme-posterior bundles resembling prior descriptions of the VOF were found in 59 out of 60 hemispheres, being absent in a single right hemisphere only. According to our results, the VOF is a 'sheet-like' bundle of fibers traveling from the postero-basal–temporal regions and basal occipital regions to the lateral gyri of the occipital cortex. We did not find strong dorsal VOF terminations within the dorsomedial portion of the occipital lobe. Dependant on how anterior the ventral terminations of the VOF were, it assumed either an oblique dorsal and posterior trajectory, or in the case of more posterior-ventral terminations, a vertical trajectory to the occipital cortex. We were able to identify the VOF as a distinct bundle, separate from the VAF in the HCP 842 (Fig. 2e, f).

Connectivity

Predominant VOF-ventral connectivity was to the SO in 87% of subjects on the left and 80% on the right. Connections to the MO were found in 37% each of subjects' right and left hemispheres, respectively. Ventrally, VOF connectivity patterns differed hemispherically. On the left, predominant ventral connectivity was to FG (80%) and inferior occipital gyrus (IO) (60%), followed by minor connectivity to the LG (30%) and ITG (23%). On the right, connectivity was spread out relative to the left, with connectivity to FG (43%), IO (40%), ITG (30%), and LG (13%) (Table 1; Fig. 2c–f).

Volumetry and lateralization

Mean left-sided VOF volume was 3.9 ml, and left-sided was 3.4 ml. This difference was not significant ($t=0.982$, $p=0.330$). In the HCP 842, left VOF volume was 1.3 ml, whilst right was 1.2 ml. Mean lateralization index was 0.1 for both subject-specific analysis and within the HCP 842, indicating both congruence of methodology and a tendency towards volumetric symmetry (Table 2).

White-matter fiber dissection results

The dissection started from the lateral surface of the hemisphere. Gyral and sulcal gray matter was removed from the precentral, postcentral, and posterior superior temporal gyri to expose underlying white matter. We preserved the gray matter of the anterior STG, and the majority of the MTG and FG to ensure visualization of VAF connectivity. We then exposed the dorsal aspect of the VAF at the SmG, noting the area where the VAF and AF proper diverged, approximately at the posterior extremity of the Sylvian fissure. On the left, we found the VAF to originate dorsally, from the SmG in both brain specimens. On the right, we noted that the VAF originated slightly more posteriorly, from the region between the SmG and AG in each specimen. Once the dorsal aspect of the VAF was exposed, we continued our dissection ventrally, removing gray and then white matter from the area below the Sylvian fissure. No connectivity of the VAF was found to the STG in any hemisphere, but, instead, ventral terminations were at the MTG bilaterally, in each of the two specimens. Once the VAF had been identified within the hemispheres, we continued our dissection posteriorly. White matter within the plane of the posterior aspect of the AF was carefully removed, to first expose the posterior-oblique aspect of the middle longitudinal fasciculus (MdLF). Fibers from the caudal aspect of the parietal portion of the MdLF were carefully removed, to expose the plane containing from

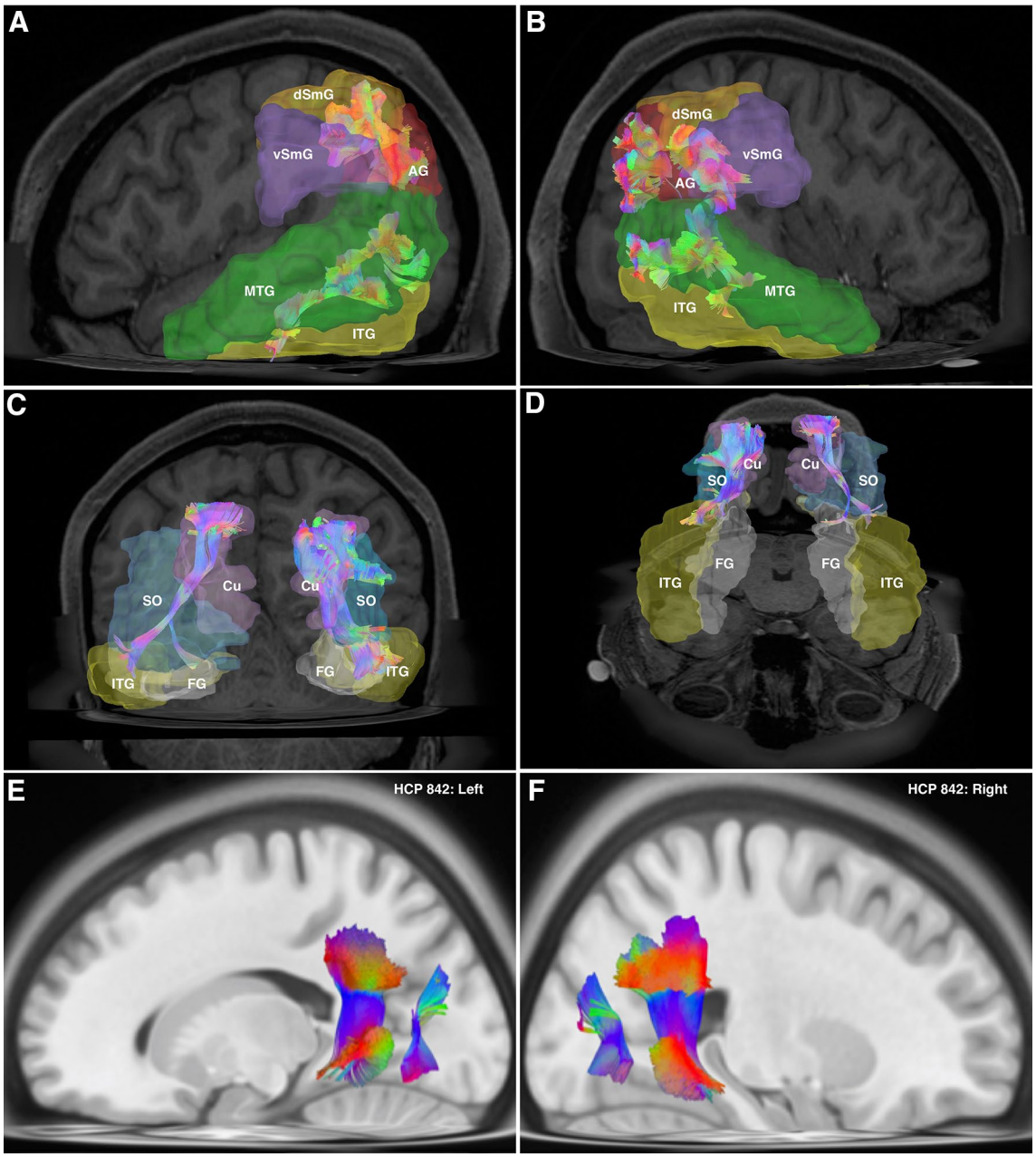

Fig. 2 **a** Sagittal view of the left hemisphere of a single subject. The AAL atlas regions corresponding to the dorsal (dSmG) and ventral (vSmG) portions of the supramarginal gyrus, angular gyrus (AG), middle temporal lobe (MTL), and inferior temporal lobe (ITL) are all labeled. Also apparent within the translucent, separate atlas regions are the dorsal and ventral connections of the left VAF throughout the parietal and temporal gyri. **b** Sagittal view of the right hemisphere of a single subject. The AAL atlas regions corresponding to the relevant connections are highlighted, and are the same as in 3A. In comparison with 3A, the figure shows more ventral and segregated nature of the parietal VAF connections. There are dense connections visible at the AG, and posterior-ventral SmG (vSmG), with negligible connectivity to the dorsal SmG (dSmG). **c** White fiber dissection picture of a subjects' left hemisphere, following removal of gray matter, U fibers, and exposure of the VAF. The red arrow indicates the angular demarcation between the AF proper and the VAF, as it passes to the dorsal aspect of the sylvian fissure (i.e., inferior parietal areas). **d** A magnified view of 3C. Orientation markers are provided at edges of the picture. The dorsal extremity of the VAF is marked by a yellow dashed-line ellipse. The ventral extremity is marked by a blue dashed-line ellipse. **e** A sagittal view of the left hemisphere of the HCP-842 atlas demonstrating both the VAF and the VOF. These individual tracts are clearly separated from each other, spatially. Tract color assignment is directional. **f** A sagittal view of the right hemisphere of the HCP-842 atlas demonstrating both the VAF and the VOF. These individual tracts are clearly separated from each other, spatially. Tract color assignment is directional

Table 1 Connectivity profiles of the VAF and VOF. Connectivity is demonstrated for superior and inferior aspects of the tract across 30 subjects. 'R' and 'L' are right and left hemispheres, respectively

	Subject	1	2	3	4	5	6	7	8	9	10	11	12
	General Notes	No R pVAF								No L pVAF			
Vertical arcuate fasciculus connectivity profiles													
Dorsal	SPL								L (A, P)				
	IPL	R (A)	L (A), R (A)	L (A)	L (A)	L (A), R (A, P)	L (A), R (A)	L (A), R (A, P)		L (A), R (A)	R (A, P)	L (A, P), R (A, P)	L (A)
	SmG	L (A), R (A)	L (A)	L (A), R (A)	R (A)	L (A), R (A)	L (A)	L (A), R (A)		R (A)	L (A), R (A)	L (A), R (A)	L (A), R (A)
	AG	L (P)	L (P), R (P)	L (P), R (P)	L (A, P), R (P)	L (P), R (P)	L (P), R (A, P)	L (P), R (A, P)	L (A), R (A, P)	R (P)	L (A, P), R (P)	R (P)	L (P), R (P)
	MO						L (P), R (P)						
Ventral	STG	R (A)								R (A)			
	MTG	L (A, P), R (A)	L (A, P)	L (A, P), R (A, P)	L (A, P), R (A, P)	L (A, P), R (A, P)	L (A, P), R (A)	L (A, P), R (A, P)	L (A), R (A, P)	L (A), R (A, P)	L (P)	L (A, P), R (A, P)	L (A), R (A, P)
	ITG		L (A, P), R (A, P)		R (P)	L (A, P), R (A, P)	R (P)	L (P)	L (P), R (A, P)	L (A), R (A, P)	L (A, P)	R (P)	L (P), R (P)
	Subject	13	14	15	16	17	18	19	20	21	22	23	24
	General Notes									No. R. VOF			
Vertical arcuate fasciculus connectivity profiles													
Dorsal	SPL												
	IPL	L (A, P), R (P)	L (A, P), R (A)	L (A)	L (A), R (A)	L (A)	L (A)	L (A, P)	L (P), R (A)	L (A, P)	L (A)	L (A)	
	SmG	L (A), R (A)	L (A)	L (A), R (A)	L (A)	L (A), R (A)	L (A, P), R (A, P)	L (A), R (A)	L (A, P), R (A)	R (A)	L (A), R (A)	L (A), R (A)	L (A), R (A)
	AG	L (P), R (P)	L (P), R (A, P)	L (P), R (P)	L (P), R (A, P)	L (P), R (A, P)		L (P), R (P)	R (A, P)	R (P)	L (A, P), R (A, P)	L (P), R (P)	L (A), R (P)
	MO												

Table 1 (continued)

	Subject	13	14	15	16	17	18	19	20	21	22	23	24
	General Notes									No. R. VOF			
Ventral	STG												
	MTG	L (A, P), R (A, P)	L (A)	L (A), R (A, P)	L (A, P), R (A, P)	L (A, P)	L (A, P), R (A, P)	L (A, P), R (A, P)	L (A, P), R (A, P)	L (A, P), R (A, P)	L (A, P), R (A, P)	L (A, P), R (P)	L (A, P), R (A)
	ITG	L (P)	L (A, P), R (A, P)	L (A, P)	L (P), R (A, P)	L (P)		L (A, P), R (P)	R (P)	R (A, P)	L (P), R (A)	L (A), R (P)	L (P), R (P)
	Subject	25	26	27	28	29	30	Connectivity (% of subjects)					
	General Notes							% L (A)	% L (P)	% R (A)	% R (P)		
Vertical arcuate fasciculus connectivity profiles													
Dorsal	SPL							3	3	0	0		
	IPL		L (A)	L (A)	R (A)		L (A)	73	20	40	17		
	SmG	R (A)	L (A, P)	L (A), R (A)	L (A)	L (A, P), R (A)	L (A), R (A)	83	13	77	3		
	AG	L (A, P), R (P)	R (A, P)	L (A, P), R (A, P)	L (A, P), R (A, P)	R (A, P)	L (A, P), R (P)	30	70	33	93		
	MO							0	3	0	3		
Ventral	STG							0	0	7	0		
	MTG	L (A, P), R (A)	L (A), R (A, P)	L (A, P), R (A, P)	L (A, P), R (A, P)	L (A, P), R (A, P)	L (A, P), R (A)	97	80	83	67		
	ITG	L (A, P), R (P)	L (A, P), R (A, P)	L (A), R (P)	R (A, P)	L (A)	L (A), R (P)	43	50	30	67		
Vertical occipital fasciculus connectivity profiles													

Table 1 (continued)

Vertical occipital fasciculus connectivity profiles													
Dorsal	SPL (ventral)		L, R										
	AG	R	L		R								
	Cun						L, R						
	SO	L, R				L, R	L, R	L	L, R	L, R	R	L, R	L, R
	MO			L	L, R	R		R			L		
Ventral	IO	L	L	L		L	R	R		L		L	
	ITG	R		L	R	R	L, R		L		L	R	
	FG	L	L, R		L	L	L, R	L, R	L, R	L, R	L		L
	LG	L			L	L	L	L	R	L	R	L	R
Vertical occipital fasciculus connectivity profiles													
Dorsal	SPL (ventral)												
	AG												
	Cun				R								
	SO	L, R	L	L, R	L, R	L, R	L, R	L, R	L, R	L	L, R	L, R	L, R
	MO	L, R	R	R	L	L, R		L, R			L, R	L, R	
Ventral	IO	R	L	L	L, R	R	L, R	R	L, R	L	L, R		L, R
	ITG	L	R					L				R	
	FG	L	L	R	L, R	L, R		L, R	L, R	L	R	L	L
	LG				L	L							
Vertical occipital fasciculus connectivity profiles						Connectivity (% of subjects)							
Dorsal	SPL (ventral)					3	3						
	AG					3	7						
	Cun	L				3	7						

Table 1 (continued)

Vertical occipital fasciculus connectivity profiles								Connectivity (% of subjects)
	SO	L, R	L, R	L, R	L, R	87	80	
	MO	L		L		37	37	
Ventral	IO	L	L, R	L	R	60	40	
	ITG	R		R	L	23	30	
	FG	L, R	L	L	L	80	43	
	LG					30	13	

'D' and 'V' represent dorsal and ventral components of the VAF, respectively. For VAF, superior terminations are within the parietal lobe, whilst inferior terminations are in the temporal lobe. For VOF, superior terminations are within the superior occipital lobe, whilst inferior terminations are within the inferior occipital lobe

SPL superior parietal lobe, *dSMG* dorsal supramarginal gyrus, *vSMG* ventral supramarginal gyrus, *AG* angular gyrus, *STG* superior temporal gyrus, *MTG* middle temporal gyrus, *ITG* inferior temporal gyrus, *Cun* cuneus, *SO* superior occipital gyrus, *MO* middle occipital gyrus, *IO* inferior occipital gyrus, *FG* fusiform gyrus, *LG* lingual gyrus

rostral-caudal: the posterior fan of the IFOF, the oblique VOF, and the ILF. This arrangement was observed in all four hemispheres (Fig. 3a–d).

Volumetric analysis of the af and slf bundles and statistical comparisons with the VAF

Across 30 subjects, the AF bundle demonstrated a mean volume of 23.9 ml on the left and 15.1 ml on the right. This hemispheric difference was highly significant ($t = 6.00$, $p < 0.01$). Likewise, mean LI across the individual subjects was 0.5, which signified very strong leftward asymmetry. For the SLF, mean volume across the 30 subjects was 17.0 ml on the left and 23.5 ml on the right. Again, this difference was highly significant ($t = -4.42$, $p < 0.01$). Mean LI across the 30 subjects was −0.3, indicating tendency towards rightward asymmetry. On the HCP-842 atlas, volume of the left AF was 19.1 ml, whilst it was 7.6 ml on the right. This corresponded to a LI of 0.9, which demonstrates extreme-leftward lateralization. The left SLF on the HCP 842 had a volume of 7.7 ml, whilst the right SLF had a volume of 12.0 ml, corresponding to a LI of −0.4. Again, this indicated strong rightward asymmetry. The one-way ANOVA comparing lateralization indices of the AF, SLF, and VAF across the 30 subjects revealed a significant difference between all three tracts [$F(2,87) = 32.69$, $p < 0.01$]. Subsequent post hoc Tukey HSD analyses between the groups revealed significant differences between the LIs of the VAF and AF ($Q = 6.62$, $p < 0.01$); the VAF and the SLF ($Q = 4.77$, $p < 0.01$); the AF and the SLF ($Q = 11.38$, $p < 0.01$).

Discussion

Vertical arcuate fasciculus

Our subject-specific and template-based connectivity analysis has demonstrated consistent reproducibility of a subdivided VAF arrangement over a range of 30 single subjects, and within an average diffusion template of 842 subjects. Interestingly and uniquely, we report that this fascicle demonstrates a characteristic dorsal–ventral manual separation pattern. There was no significant difference between the right and left vVAF connectivity profiles, and we can infer that both are substantial conduits between the SmG and MTG, with the left vVAF also preferentially serving SMG–MTG connectivity. Likewise, the dVAF is a conduit between the AG and MTG/ITG. Broadly, our description of VAF connectivity fits with the previous descriptions of the 'posterior-AF' (Catani et al. 2005; Fernández-Miranda et al. 2008; Martino et al. 2013b). Our results also concur with those of Martino et al. (2013), in response to Bartsch et al. (2013), demonstrating that this temporo-parietal component

Table 2 Table of volumetric information of the VAF, VOF, AF, and SLF across 30 subjects and within the HCP 842. VAF volumes are divided into left and right, ventral (vVAF) and dorsal (dVAF)

	Subject		1	2	3	4	5	6	7	8	9	10	11	12	13	14	15	16
	General notes		No R pVAF								No L pVAF							
Vertical arcuate fasciculus volumetry																		
VAF volumes	L aVAF		6.5	7.9	7.0	5.5	9.3	4.1	4.3	9.3	5.5	3.5	5.8	7.1	5.3	6.9	9.8	3.3
	L pVAF		2.6	2.8	0.7	1.4	1.3	5.1	3.5	1.9	0.0	1.9	1.3	2.0	5.9	4.9	5.4	6.6
	R aVAF		5.5	3.8	1.6	1.9	12.5	5.7	8.2	2.7	9.0	7.0	2.9	4.6	2.9	5.9	5.8	3.9
	R pVAF		0.0	4.0	2.1	4.1	3.6	6.5	3.6	1.7	2.3	2.0	8.0	5.5	9.9	3.5	4.1	5.2
	L (aVAF + pVAF)		9.1	10.7	7.7	6.8	10.6	9.2	7.8	11.2	5.5	5.4	7.1	9.1	11.2	11.7	15.1	9.9
	R (aVAF + pVAF)		5.5	7.8	3.7	6.0	16.2	12.2	11.8	4.4	11.3	9.1	10.9	10.2	12.9	9.4	9.9	9.1
	L pre-separation		8.6	10.7	7.6	6.8	10.5	9.2	9.4	11.2	5.5	5.0	6.4	9.0	10.8	10.9	14.9	9.4
	R pre-seperation		5.5	7.7	3.6	6.0	15.8	12.2	11.1	4.3	10.8	8.9	10.3	9.9	11.3	9.0	9.5	8.5
	Difference L		0.5	0.0	0.2	0.0	0.0	0.0	− 1.6	0.0	0.0	0.4	0.7	0.1	0.4	0.8	0.2	0.5
	Difference R		0.0	0.1	0.0	0.0	0.3	0.0	0.7	0.1	0.5	0.1	0.6	0.3	1.6	0.4	0.5	0.6
	LI pre-separation		0.5	0.3	0.7	0.1	− 0.4	− 0.3	− 0.4	0.9	− 0.7	− 0.5	− 0.4	− 0.1	− 0.1	0.2	0.4	0.1
	LI (ant. + post.)		0.4	0.3	0.7	0.1	− 0.4	− 0.3	− 0.2	0.9	− 0.6	− 0.6	− 0.5	− 0.1	0.0	0.2	0.4	0.1
Vertical occipital fasciculus volumetry																		
VOF volumes	Vol L		2.7	3.2	1.1	3.1	2.5	4.2	2.1	2.0	2.3	3.6	5.1	2.8	3.7	2.4	2.0	6.3
	Vol R		5.6	1.0	1.3	3.4	4.4	3.1	2.6	3.2	0.8	0.8	3.5	1.7	2.5	5.4	3.4	7.2
	LI		− 0.7	1.1	− 0.1	− 0.1	− 0.5	0.3	− 0.2	− 0.5	0.9	1.3	0.4	0.5	0.4	− 0.8	− 0.5	− 0.1
Adjacent fascicles																		
AF volumes	L AF		23.1	27.2	21.7	20.8	24.2	22.5	26.7	24.4	26.4	36.9	18.5	24.1	19.2	31.8	21.0	26.8
	R AF		17.6	16.8	16.9	15.3	14.3	11.9	18.7	21.8	7.9	15.4	8.6	26.8	7.3	9.5	11.5	23.3
	LI		0.3	0.5	0.2	0.3	0.5	0.6	0.4	0.1	1.1	0.8	0.7	− 0.1	0.9	1.1	0.6	0.1
SLF volumes	L SLF		23.2	16.8	17.9	14.9	19.4	13.1	19.1	15.8	15.3	24.5	12.8	20.0	14.1	15.2	11.2	20.7
	R SLF		28.7	29.7	21.9	20.9	24.2	23.1	25.2	22.2	17.1	39.0	17.1	24.6	22.5	29.5	20.1	33.2
	LI		− 0.2	− 0.6	− 0.2	− 0.3	− 0.2	− 0.6	− 0.3	− 0.3	− 0.1	− 0.5	− 0.3	− 0.2	− 0.5	− 0.6	− 0.6	− 0.5

	Subject	17	18	19	20	21	22	23	24	25	26	27	28	29	30	Mean	HCP 842
	General notes					No. R. VOF											
Vertical arcuate fasciculus volumetry																	
VAF volumes	L aVAF	5.7	6.4	9.8	2.9	3.4	5.0	10.2	3.8	5.1	5.2	9.5	4.2	7.2	8.3	6.3	3.9
	L pVAF	9.1	5.4	5.6	3.9	5.3	3.7	3.2	4.2	4.7	2.6	4.3	6.8	2.2	6.6	3.8	2.8
	R aVAF	8.3	3.2	4.8	4.4	7.5	9.7	3.0	6.5	6.8	5.8	6.7	2.9	3.0	3.3	5.3	2.1
	R pVAF	4.8	4.7	6.2	6.8	7.5	1.7	2.5	3.1	5.7	3.9	6.1	5.5	2.8	5.4	4.4	4.8

Table 2 (continued)

	Subject General notes	17	18	19	20	21 No. R. VOF	22	23	24	25	26	27	28	29	30	Mean	HCP 842
	L (aVAF + pVAF)	14.8	11.8	15.4	6.9	8.7	8.7	13.4	8.0	9.8	7.8	13.8	11.0	9.4	14.8	10.1	6.7
	R (aVAF + pVAF)	13.0	7.9	11.0	11.1	15.0	11.4	5.5	9.6	12.5	9.6	12.8	8.5	5.8	8.7	9.8	6.9
	L pre-separation	14.7	10.2	14.2	5.6	7.0	8.5	12.9	8.0	9.3	7.3	13.2	10.5	8.5	14.8	9.7	5.9
	R pre-seperation	12.9	7.8	10.3	10.3	12.3	11.3	5.5	9.6	12.5	8.9	12.8	7.7	5.3	8.7	9.3	6.7
	Difference L	0.1	1.6	1.2	1.3	1.7	0.2	0.5	0.0	0.5	0.4	0.6	0.5	0.9	0.1	0.4	0.8
	Difference R	0.2	0.0	0.7	0.8	2.7	0.1	0.0	0.1	0.0	0.8	0.0	0.8	0.5	0.0	0.4	0.1
	LI pre-separation	0.1	0.4	0.3	− 0.5	− 0.5	− 0.3	0.8	− 0.2	− 0.2	− 0.2	0.1	0.3	0.5	0.5	0.0	0.0
	LI (ant. + post.)	0.1	0.3	0.3	− 0.6	− 0.5	− 0.3	0.8	− 0.2	− 0.3	− 0.2	0.0	0.3	0.5	0.5	0.0	− 0.1
Vertical occipital fasciculus volumetry																	
VOF volumes	Vol L	5.0	3.2	9.7	3.5	2.8	4.5	7.8	3.3	1.1	4.8	1.8	4.8	8.4	7.0	3.9	1.3
	Vol R	5.4	4.3	3.8	4.7	0.0	4.3	5.2	2.6	2.1	4.3	6.9	3.1	3.5	1.7	3.4	1.2
	LI	− 0.1	− 0.3	0.9	− 0.3	2.0	0.0	0.4	0.2	− 0.6	0.1	− 1.2	0.4	0.8	1.2	0.1	0.1
Adjacent fascicles																	
AF volumes	L AF	14.9	31.0	25.4	21.6	17.0	20.2	22.5	30.8	20.2	24.0	21.9	22.3	19.2	30.8	23.9	19.1
	R AF	11.9	22.1	9.6	7.1	4.7	5.8	15.1	26.9	25.8	18.3	8.3	19.7	12.6	20.6	15.1	7.6
	LI	0.2	0.3	0.9	1.0	1.1	1.1	0.4	0.1	− 0.2	0.3	0.9	0.1	0.4	0.4	0.5	0.9
SLF volumes	L SLF	15.8	19.7	13.7	20.6	17.9	13.9	21.1	13.9	23.6	15.1	13.5	18.5	15.9	12.8	17.0	7.7
	R SLF	26.7	8.6	11.4	27.8	15.3	12.3	28.9	40.8	23.2	21.9	21.9	23.8	18.1	24.1	23.5	12.0
	LI	− 0.5	0.8	0.2	− 0.3	0.2	0.1	− 0.3	− 1.0	0.0	− 0.4	− 0.5	− 0.3	− 0.1	− 0.6	− 0.3	− 0.4

The summated volumes are when the separate ventral and dorsal components are added together, whilst the pre-separation values are taken for the VAF as a whole, before they were separated. Difference is the value when the pre-separation values are subtracted from summated values (i.e., vVAF + dVAF). This gives a volumetric result representing the degree of overlapping between the ventral and dorsal sums. LI pre-separation is the LI of the entire PAT prior to separating it into its dorsal and ventral components, whilst LI (vVAF + dVAF) represents the LI calculated from the added dorsal and ventral VAF volumes

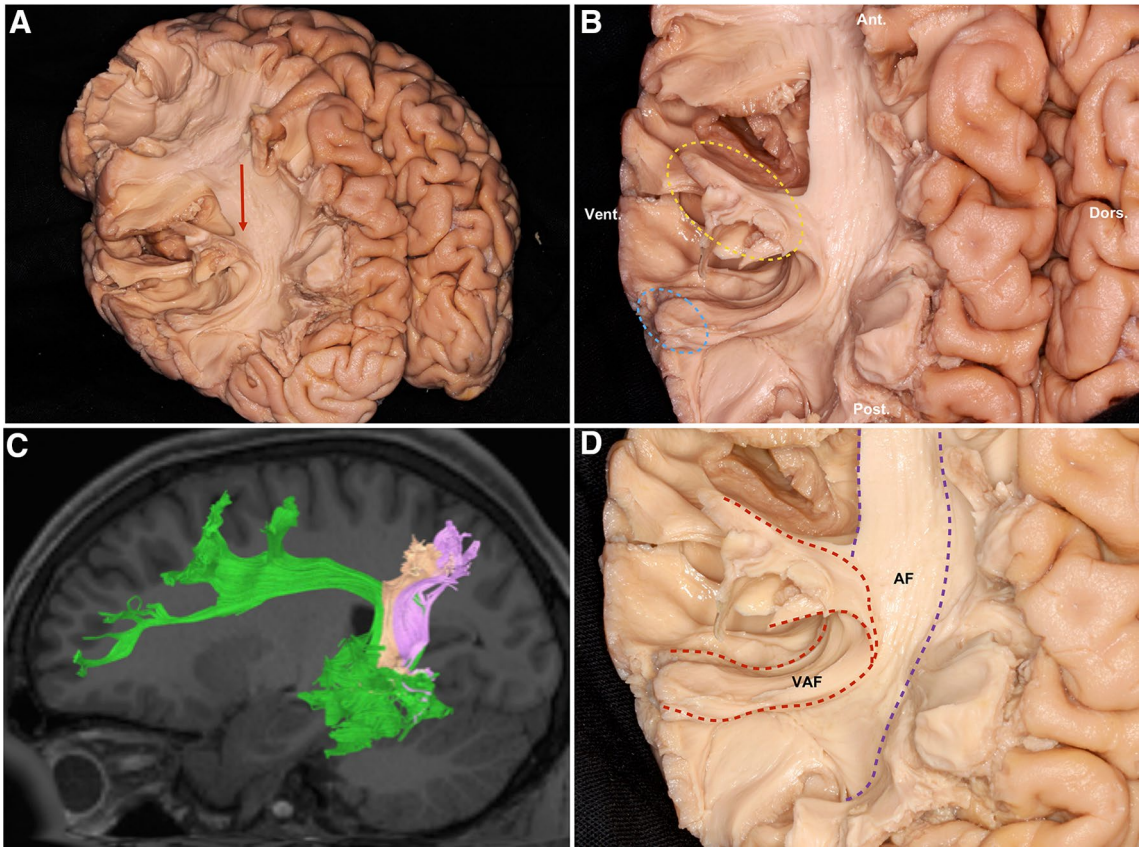

Fig. 3 **a** A supero-lateral view of a post-mortem specimen. The left hemispheric cortex and superficial white matter have been removed to expose the VAF and AF. The parietal diversion of AF and VAF is readily apparent and is demarcated by a red arrow. **b** A magnified view of 5A. Orientation guides are included at the borders of the picture: anterior (ant.), posterior (post.), ventral (vent.), and dorsal (dors.). The dorsal (parietal) terminations of the VAF are visible and highlighted by a yellow broken ellipse. The ventral (temporal) terminations of the VAF are visible and highlighted by a blue broken ellipse. **c** A tractographic representation showing the specific relationship between the AF and the VAF. Clearly visible is the VAF (dorsal—pink; ventral—light orange) lying superficial to the AF proper (green). The temporal terminations of the VAF are obscured by the upslanting of the AFs temporal terminations. **d** A magnified view of the left hemisphere from another post-mortem specimen. The parietal divergence of the AF (purple broken lines) and VAF (red broken lines) is indicated by colored broken lines

is the most lateral of the association fasciculi in this region, and that the VAF is spatially distinct from the VOF. As we did not specifically look into the 'temporor-parieto-occipital (TPO)' component in this study, we cannot say with absolute certainty whether the TPO component is a distinct bundle of fibers as postulated by Kamali et al. and Wu et al. or instead comprised of either (a) U-fibers or (b) components from other from other close-proximity systems. This is an issue requiring further investigation. Our volumetric analysis revealed no indication of VAF hemispheric lateralization, instead, showing symmetrical volumetric tendency. When volumetry differences between the VAF, the AF and the SLF are taken in context, results can be considered further evidence of the VAF as dissociated from both the AF and SLF. If the VAF was part of the same system as the AF, it would be expected to show the extreme-leftward-dominant volumetry according to evolutionary theories (Rilling et al. 2008; Glasser and Rilling 2008; Fernández-Miranda et al. 2015), as the AF. Furthermore, if the VAF was associated with the SLF system, it would be expected to show the strong rightward-dominant asymmetry of the latter. As such, our results suggest that the VAF is instead an independent fiber system, unique from both the parieto-frontal SLF and temporo-frontal AF.

Based on our present data, and our previous studies into the AF and SLF, we believe the 'perisylvian-SLF' view to be anatomically questionable. This view has likely been propagated due to the inability of DTI to differentiate between close-proximity crossing fiber systems at an adequate angular resolution. The misclassification of VAF with the other dorsal systems may have resulted from its shared connectivity profiles with the SLF dorsally, and AF ventrally. Continuing to regard the AF as a 'tripartite' system with a vertical component defies its actual contemporary 'dorsal–ventral'

morphology and may further confuse understanding. In accordance with the current terminology and to reconcile some controversy, we propose the term 'temporo-parietal aslant tract' (TPAT) to more accurately describe the previously defined 'VAF.' We henceforth describe the VAF and its components as the dorsal TPAT (dTPAT) and ventral TPAT (vTPAT).

The temporo-parietal aslant tract: a distinct structural and functional entity

To further complicate matters, recent tractography studies have demonstrated a so-called 'temporo-parieto-occipital' (TPO) connection, distinct from the TPAT/SLF-V. Kamali et al. (2014a, b), using DTI, found a connection between the posterior temporal lobe and the superior parietal lobule. Another recent, non-tensor study into short, vertical temporo-parietal connections by Wu et al. (2016) claimed also to find this novel 'TPO' connection, in addition to the previously described 'SLF-V' (i.e., the TPAT). These fibers are described as arising from the baso-lateral temporal areas and travel vertically, between the 'vertical' leg of the AF proper, and the TPAT superficially, before terminating at the superior parietal cortex. We did not locate a distinct bundle resembling the TPO during our tractographic or dissection study; nevertheless, the TPO and its existence among the posterior vertical fibers should be further explored. We consistently demonstrated the unique, dorsal–ventral TPAT structure bi-hemispherically over a range of 30 subjects, and we have also shown that this structure is preserved within the large volume HCP-842 atlas (Yeh et al. 2018) [larger than the NTU-90 used by Wu et al. (2016)]. Our study, instead, demonstrates the 'SLF-V', i.e., the TPAT is, indeed, an independent bundle of fibers, with distinctive dorsal–ventral subdivision patterns, connectivity profiles, and volumetric lateralization. Wu et al. (2016) also propose that 'supramarginal' and 'angular' divisions of SLF-V which we believe are consistent with our dTPAT and vTPAT nomenclature.

Functionally, the dominant vTPAT, which demonstrated preferential SmG–MTG connectivity, may, therefore, serve as a conduit for mapping sounds or read words to their meanings, the latter function potentially being subserved by MTG (Acheson and Hagoort 2013). Furthermore, ischemia to cortex of the dominant SmG has been directly implicated in word repetition deficits (Fridriksson et al. 2010). The authors of the study implicated the 'posterior-AF' in the observed conduction deficits. Whether they were referring specifically to the morphological entity synonymous with the TPAT is uncertain; however, we can infer that the TPAT, and vTPAT specifically, is implicated in this task, from its connectivity to the inferior parietal regions. As for the dTPAT, its rightward-preferential AG-MTG/ITG connectivity may thus subserve roles in visuospatially locating objects in a 3D space. Our reasoning is based upon functional imaging studies implicating the right AG in 'action-awareness (Farrer et al. 2008)' and right MTG/ITG in object-location memory (Milner 1997; Waberski et al. 2001).

Vertical occipital fasciculus

Despite lack of a concise anatomical description of an occipital vertical white-matter fascicle, clinical evidence demonstrating alexia resulting from damage to occipital white matter indicated its existence. These pre-tractographic clinical data were complemented by the tractographic description of VOF anatomy (Catani et al. 2002; Wakana et al. 2004), showing a thin sheet of vertically ascending fibers lateral to the white matter of the sagittal stratum. It was not until 2013; however, that Yeatman et al. in a series of dedicated studies offered a specific elaboration of VOF structure and function. They described a tract originating from the occipito-temporal sulcus ascending vertically, lateral to the ILF and inferior fronto-occipital fasciculus, terminating in the lateral occipital and inferior parietal lobes. We further elaborate upon this description with our connectivity analysis, showing a leftward-lateralized pattern of connectivity from the FG and ITG to the lateral occipital cortices (i.e., SO and MO). A 2014 functional study (Bouhali et al. 2014) indicated leftward lateralization of visual word-form area (VWA) connectivity to the dorsal parieto-occipital regions. Though our results are generally congruent with this postulation, the authors of this study demonstrated that the VWA was functionally associated with perisylvian language areas. Our results do not support their latter proposition, however, as neither the TPAT nor the VOF shows FG-perisylvian connectivity. A combined functional–tractographic study by Takemura et al. (2016) specifically implicated the VOF in communication between dorsal (V3A/B) and ventral (hV4/VO-1) visual areas. Our connectivity results showing the VOF as a conduit between ventrolateral and dorsolateral posterior-occipital areas are consistent with the proposed specialization of these cortical areas (DeYoe et al. 1996), and, thus, further reinforce the proposal of Takemura et al. (2016).

Technical considerations and limitations

Weiner et al. (2016) illustrated the potential difficulty of distinguishing between the TPAT and the VOF tractographically, especially using DTI. Our results demonstrate that, using HCPs high-spatial and high-angular-resolution data, the VAF and VOF are consistently reproduced as spatially separated fiber bundles. Our results serve to reinforce suggestions by Weiner et al. (2016), highlighting the necessity for accurate, high-resolution tractography methods to delineate

close-proximity systems. It is likely that the controversy regarding the dissociation of TPAT and VOF likely arose due to the tractographic artifact that has been, otherwise, referred to as the 'TPO' component. There may be additional U fibers that contribute to the notion of a 'bridge' between the TPAT and VOF, but further investigation is required. Furthermore, using our HCP 842 atlas (Yeh et al. 2018), we can definitively address the question of VOF and TPAT separation. We highlight the necessity for a high index of suspicion in discerning false continuations from meaningful tracts. Though scientific rigor would support the inclusion of 'all' generated fibers from seeds/ROIs in analyses and subsequent classification of fiber systems, one must consider the 'signal-to-noise' concept when using this technique: The proportion of false continuations to real tracts may indicate artificial connective and volumetric profiles. A thorough knowledge of neuroanatomy is, thus, essential when conducting tractography.

Conclusions

Our tractography and dissection-based study into the anatomy of the VAF have demonstrated that this short, vertical temporo-parietal tract can be subdivided into anterior and posterior divisions. Furthermore, we have demonstrated connective lateralization but the volumetric symmetry of this system. Our evidence serves to reinforce an idea that the VAF is a distinct fasciculus, independent of the AF and SLF systems. We, therefore, propose a new name for this tract: Temporo-parietal Aslant Tract, in line with the current nomenclature and as an anatomical analog to its frontal counterpart. Second, we have demonstrated that the parietal aslant and VOF are distinct, spatially separated systems, each demonstrating variable connectivity and probable functional specialization.

Compliance with ethical standards

Conflict of interest The authors report no conflicts of interest.

References

Acheson DJ, Hagoort P (2013) Stimulating the brain's language network: syntactic ambiguity resolution after TMS to the inferior frontal gyrus and middle temporal gyrus. J Cogn Neurosci 25:1664–1677. https://doi.org/10.1162/jocn_a_00430

Bartsch AJ, Geletneky K, Jbabdi S (2013) The temporoparietal fiber intersection area and wernicke perpendicular fasciculus. Neurosurgery 73:E381–E382. https://doi.org/10.1227/01.neu.0000430298.25585.1d

Bouhali F, Thiebaut de Schotten M, Pinel P et al (2014) Anatomical connections of the visual word form area. J Neurosci Off J Soc Neurosci 34:15402–15414. https://doi.org/10.1523/JNEUROSCI.4918-13.2014

Catani M, Thiebaut de Schotten M (2008) A diffusion tensor imaging tractography atlas for virtual in vivo dissections. Cortex J Devoted Study Nerv Syst Behav 44:1105–1132. https://doi.org/10.1016/j.cortex.2008.05.004

Catani M, Howard RJ, Pajevic S, Jones DK (2002) Virtual in vivo interactive dissection of white matter fasciculi in the human brain. NeuroImage 17:77–94. https://doi.org/10.1006/nimg.2002.1136

Catani M, Jones DK, ffytche DH (2005) Perisylvian language networks of the human brain. Ann Neurol 57:8–16. https://doi.org/10.1002/ana.20319

Catani M, Dell'acqua F, Vergani F et al (2012) Short frontal lobe connections of the human brain. Cortex J Devoted Study Nerv Syst Behav 48:273–291. https://doi.org/10.1016/j.cortex.2011.12.001

Catani M, Mesulam MM, Jakobsen E et al (2013) A novel frontal pathway underlies verbal fluency in primary progressive aphasia. Brain J Neurol 136:2619–2628. https://doi.org/10.1093/brain/awt163

DeYoe EA, Carman GJ, Bandettini P et al (1996) Mapping striate and extrastriate visual areas in human cerebral cortex. Proc Natl Acad Sci U S A 93:2382–2386

Farquharson S, Tournier J-D, Calamante F et al (2013) White matter fiber tractography: why we need to move beyond DTI. J Neurosurg 118:1367–1377. https://doi.org/10.3171/2013.2.JNS121294

Farrer C, Frey SH, Horn V et al (2008) The Angular Gyrus Computes Action Awareness Representations. Cereb Cortex 18:254–261. https://doi.org/10.1093/cercor/bhm050

Fernández-Miranda JC, Rhoton AL, Alvarez-Linera J et al (2008) Three-dimensional microsurgical and tractographic anatomy of the white matter of the human brain. Neurosurgery 62:989–1026. https://doi.org/10.1227/01.neu.0000333767.05328.49 **(discussion 1026–1028)**

Fernández-Miranda JC, Wang Y, Pathak S et al (2015) Asymmetry, connectivity, and segmentation of the arcuate fascicle in the human brain. Brain Struct Funct 220:1665–1680. https://doi.org/10.1007/s00429-014-0751-7

Fridriksson J, Kjartansson O, Morgan PS et al (2010) Impaired Speech Repetition and Left Parietal Lobe Damage. J Neurosci 30:11057–11061. https://doi.org/10.1523/JNEUROSCI.1120-10.2010

Glasser MF, Rilling JK (2008) DTI tractography of the human brain's language pathways. Cereb Cortex N Y N 18:2471–2482. https://doi.org/10.1093/cercor/bhn011

Güngör A, Baydin S, Middlebrooks EH et al (2017) The white matter tracts of the cerebrum in ventricular surgery and hydrocephalus. J Neurosurg 126:945–971. https://doi.org/10.3171/2016.1.JNS152082

Kamali A, Flanders AE, Brody J et al (2014a) Tracing superior longitudinal fasciculus connectivity in the human brain using high resolution diffusion tensor tractography. Brain Struct Funct 219:269–281. https://doi.org/10.1007/s00429-012-0498-y

Kamali A, Sair HI, Radmanesh A, Hasan KM (2014b) Decoding the superior parietal lobule connections of the superior longitudinal fasciculus/arcuate fasciculus in the human brain. Neuroscience 277:577–583. https://doi.org/10.1016/j.neuroscience.2014.07.035

Keser Z, Ucisik-Keser FE, Hasan KM (2016) Quantitative mapping of human brain vertical-occipital fasciculus. J Neuroimaging Off J Am Soc Neuroimaging 26:188–193. https://doi.org/10.1111/jon.12268

Lawes INC, Barrick TR, Murugam V et al (2008) Atlas-based segmentation of white matter tracts of the human brain using diffusion tensor tractography and comparison with classical dissection. NeuroImage 39:62–79. https://doi.org/10.1016/j.neuroimage.2007.06.041

Martino J, De Lucas EM (2014) Subcortical anatomy of the lateral association fascicles of the brain: a review. Clin Anat N Y N 27:563–569. https://doi.org/10.1002/ca.22321

Martino J, García-Porrero JA (2013) Wernicke perpendicular fasciculus and vertical portion of the superior longitudinal fasciculus: in

reply. Neurosurgery 73:E382–E383. https://doi.org/10.1227/01.neu.0000430303.56079.0e

Martino J, da Silva-Freitas R, Caballero H et al (2013a) Fiber dissection and diffusion tensor imaging tractography study of the temporoparietal fiber intersection area. Neurosurgery 72:87–97. https://doi.org/10.1227/NEU.0b013e318274294b discussion 97–98.

Martino J, De Witt Hamer PC, Berger MS et al (2013b) Analysis of the subcomponents and cortical terminations of the perisylvian superior longitudinal fasciculus: a fiber dissection and DTI tractography study. Brain Struct Funct 218:105–121. https://doi.org/10.1007/s00429-012-0386-5

Milner AD (1997) Vision without knowledge. Philos Trans R Soc Lond B Biol Sci 352:1249–1256. https://doi.org/10.1098/rstb.1997.0107

Panesar SS, Yeh F-C, Deibert CP et al (2017) A diffusion spectrum imaging-based tractographic study into the anatomical subdivision and cortical connectivity of the ventral external capsule: uncinate and inferior fronto-occipital fascicles. Neuroradiology 59:971–987. https://doi.org/10.1007/s00234-017-1874-3

Rilling JK, Glasser MF, Preuss TM et al (2008) The evolution of the arcuate fasciculus revealed with comparative DTI. Nat Neurosci 11:426–428. https://doi.org/10.1038/nn2072

Takemura H, Rokem A, Winawer J et al (2016) A major human white matter pathway between dorsal and ventral visual cortex. Cereb Cortex N Y N 26:2205–2214. https://doi.org/10.1093/cercor/bhv064

Takemura H, Pestilli F, Weiner KS et al (2017) Occipital white matter tracts in human and macaque. Cereb Cortex N Y N 27:3346–3359. https://doi.org/10.1093/cercor/bhx070

Thiebaut de Schotten M, Ffytche DH, Bizzi A et al (2011) Atlasing location, asymmetry and inter-subject variability of white matter tracts in the human brain with MR diffusion tractography. NeuroImage 54:49–59. https://doi.org/10.1016/j.neuroimage.2010.07.055

Tzourio-Mazoyer N, Landeau B, Papathanassiou D et al (2002) Automated anatomical labeling of activations in SPM using a macroscopic anatomical parcellation of the MNI MRI single-subject brain. NeuroImage 15:273–289. https://doi.org/10.1006/nimg.2001.0978

Waberski TD, Kreitschmann-Andermahr I, Kawohl W et al (2001) Spatio-temporal source imaging reveals subcomponents of the human auditory mismatch negativity in the cingulum and right inferior temporal gyrus. Neurosci Lett 308:107–110. https://doi.org/10.1016/S0304-3940(01)01988-7

Wang X, Pathak S, Stefaneanu L et al (2016) Subcomponents and connectivity of the superior longitudinal fasciculus in the human brain. Brain Struct Funct 221:2075–2092. https://doi.org/10.1007/s00429-015-1028-5

Weiner KS, Yeatman JD, Wandell BA (2017) The posterior arcuate fasciculus and the vertical occipital fasciculus. Cortex J Devoted Study Nerv Syst Behav 97:274–276. https://doi.org/10.1016/j.cortex.2016.03.012

Wu Y, Sun D, Wang Y et al (2016) Tracing short connections of the temporo-parieto-occipital region in the human brain using diffusion spectrum imaging and fiber dissection. Brain Res 1646:152–159. https://doi.org/10.1016/j.brainres.2016.05.046

Yeatman JD, Rauschecker AM, Wandell BA (2013) Anatomy of the visual word form area: adjacent cortical circuits and long-range white matter connections. Brain Lang 125:146–155. https://doi.org/10.1016/j.bandl.2012.04.010

Yeatman JD, Weiner KS, Pestilli F et al (2014) The vertical occipital fasciculus: a century of controversy resolved by in vivo measurements. Proc Natl Acad Sci U S A 111:E5214–E5223. https://doi.org/10.1073/pnas.1418503111

Yeh F-C, Tseng W-YI (2011) NTU-90: a high angular resolution brain atlas constructed by q-space diffeomorphic reconstruction. NeuroImage 58:91–99. https://doi.org/10.1016/j.neuroimage.2011.06.021

Yeh F-C, Wedeen VJ, Tseng W-YI (2010) Generalized q-sampling imaging. IEEE Trans Med Imaging 29:1626–1635. https://doi.org/10.1109/TMI.2010.2045126

Yeh F-C, Verstynen TD, Wang Y et al (2013) Deterministic diffusion fiber tracking improved by quantitative anisotropy. PloS One 8:e80713. https://doi.org/10.1371/journal.pone.0080713

Yeh F-C, Panesar S, Fernandes D et al (2018) Population-averaged atlas of the macroscale human structural connectome and its network topology. NeuroImage 178:57–68. https://doi.org/10.1016/j.neuroimage.2018.05.027